Drug Delivery and Translational Research (2023) 13:1128–1139
https://doi.org/10.1007/s13346-022-01278-4

ORIGINAL ARTICLE

Improving in vivo oral bioavailability of a poorly soluble drug: a case study on polymeric versus lipid nanoparticles

Giovanna Rassu[1,2] · Antonella Obinu[1] · Carla Serri[2] · Sandra Piras[1,2] · Antonio Carta[1,2] · Luca Ferraro[3] · Elisabetta Gavini[1,2] · Paolo Giunchedi[1,2] · Alessandro Dalpiaz[4]

Accepted: 1 December 2022 / Published online: 12 December 2022

Abstract

Poorly soluble drugs must be appropriately formulated for clinical use to increase the solubility, dissolution rate, and permeation across the intestinal epithelium. Polymeric and lipid nanocarriers have been successfully investigated for this aim, and their physicochemical properties, and in particular, the surface chemistry, significantly affect the pharmacokinetics of the drugs after oral administration. In the present study, PLGA nanoparticles (SS13NP) and solid lipid nanoparticles (SS13SLN) loaded with SS13, a BCS IV model drug, were prepared. SS13 bioavailability following the oral administration of SS13 (free drug), SS13NP, or SS13SLN was compared. SS13NP had a suitable size for oral administration (less than 300 nm), a spherical shape and negative zeta potential, similarly to SS13SLN. On the contrary, SS13NP showed higher physical stability but lower encapsulation efficiency (54.31 ± 6.66%) than SS13SLN (100.00 ± 3.11%). When orally administered (0.6 mg of drug), SS13NP showed higher drug AUC values with respect to SS13SLN (227 ± 14 versus 147 ± 8 µg/mL min), with higher C_{max} (2.47 ± 0.14 µg/mL versus 1.30 ± 0.15 µg/mL) reached in a shorter time (20 min versus 60 min). Both formulations induced, therefore, the oral bioavailability of SS13 (12.67 ± 1.43% and 4.38 ± 0.39% for SS13NP and SS12SLN, respectively) differently from the free drug. These in vivo results confirm that the chemical composition of nanoparticles significantly affects the in vivo fate of a BCS IV drug. Moreover, PLGA nanoparticles appear more efficient and rapid than SLN in allowing drug absorption and transport to systemic circulation.

Keywords Poorly soluble drug · BCS IV drug · Oral bioavailability · PLGA nanoparticle · SLN

Introduction

It was estimated that poorly water-soluble drugs represent about 90% of drugs in the stage of development and approximately 40% of those in the market, of which 80% are orally administered [1]. Poor water solubility affects their oral bioavailability, which is low and inconsistent, and consequently, their therapeutic response that is linked to non-optimal dosage [2]. Based on the biopharmaceutical classification system (BCS), these drugs are categorized in II (low

✉ Giovanna Rassu
grassu@uniss.it

Antonella Obinu
aobinu@uniss.it

Carla Serri
cserri@uniss.it

Sandra Piras
piras@uniss.it

Antonio Carta
acarta@uniss.it

Luca Ferraro
frl@unife.it

Elisabetta Gavini
eligav@uniss.it

Paolo Giunchedi
pgiunc@uniss.it

Alessandro Dalpiaz
dla@unife.it

1 Department of Chemistry and Pharmacy, University of Sassari, via Muroni 23/a, 07100 Sassari, Italy

2 Department of Medicine, Surgery and Pharmacy, University of Sassari, viale San Pietro 43/B, 07100 Sassari, Italy

3 Department of Life Sciences and Biotechnology, University of Ferrara, via Borsari 46, 44121 Ferrara, Italy

4 Department of Chemical, Pharmaceutical and Agricultural Sciences, University of Ferrara, via Fossato di Mortara 19, 44121 Ferrara, Italy

solubility and high permeability) and IV (low solubility and low permeability) classes depending on in vivo absolute bioavailability or in vitro Caco-2 cell studies [3]. Both BCS II and IV compounds must be appropriately formulated for optimal clinical efficacy. The BCS II drugs require formulative strategies to increase the solubility in gastrointestinal (GI) fluids and the dissolution rate; this is not enough for those of the BCS IV class, for which it is necessary to design drug delivery systems capable of increasing the drug permeation across the intestinal epithelium [4].

The nanoparticle technology has been widely used for these purposes (nanocrystal, nanoemulsion, lipid, and polymeric nanoparticles) [2, 4–8]. In particular, it shows different benefits like fast and efficient processes, enhanced bioavailability, and potential clinical application [2]. Nevertheless, the physicochemical properties of the nanocarriers significantly affect the pharmacokinetics of the drugs after oral administration [6, 9]. The size, shape, surface properties, and chemical composition are key factors affecting intestinal absorption and biodistribution to a greater extent than drug properties [2, 6, 9, 10]. The size affects the diffusion through the mucus layer and the cellular uptake, which increases as the size decreases [6, 10, 11]. The cellular uptake and retention time in the GI tract also depend on nanoparticle shape that influences the interaction and adhesion with the membrane of enterocytes and villi [6, 11]: rod-shaped nanoparticles are more effective than spheres, thanks to the larger surface area [11]. Nevertheless, the surface chemistry of nanoparticles has a significant impact on the pharmacokinetics and pharmacodynamics of the loaded drugs [6, 9–11].

Polymeric and lipid materials have been successfully investigated for the preparation of oral nanocarriers for poorly soluble drugs [8, 10, 12–14], but from the literature data, it is not possible to establish a priori the optimal carrier for the oral delivery of a BCS IV drug.

In the present study, polymeric and lipid nanoparticles loaded with SS13 were orally administered to rats to compare their pharmacokinetic profiles. SS13, a phenoxymethylquinoxaline newly synthesized, was selected as a BCS IV model drug due to its insolubility in simulated GI media, the low Log *P* value (0.817 ± 0.031), and the inability to pass through the excised intestinal mucosa [12]. In particular, poly (lactic-co-glycolic acid) (PLGA) nanoparticles were prepared and characterized before in vivo studies for obtaining nanoparticles with size and morphology comparable with those of solid lipid nanoparticles (SLN), previously reported [12] to exclude the influence of other factors besides the composition.

PLGA was selected because extensively used for preparing nano drug delivery systems [15]; it is biocompatible, biodegradable, safe, and approved by the regulatory agencies (FDA and EMA). In particular, PLGA nanoparticles containing poly/vinyl alcohol (PVA) as an emulsifier/stabilizer were capable of increasing the in vivo oral bioavailability of poorly soluble drugs [14, 16, 17]. Similarly, SLN are biocompatible, biodegradable, non-toxic, and enhance the oral bioavailability of different molecules [8, 18, 19]. Witepsol-based SLN are promising nanocarriers for oral delivery [12, 20], mainly when Gelucire is added due to its absorption enhancer properties [21].

Methods

Materials

SS13, a novel phenoxymethylquinoxaline derivative, was synthesized at Medicinal Chemistry Laboratory at the University of Sassari [12]. Poly(D,L-lactide-co-glycolide) (PLGA) (Resomer RG 503, lactide:glycolide 50:50, ester terminated, M_w 24.000–38.000), poly/vinyl alcohol (PVA) (87–90% hydrolyzed, M_w 30.000–70.000), dichloromethane (DCM), phosphate-buffered saline (PBS, NaCl 0.138 M; KCl 0.0027 M; pH7.4, at 25 °C), Krebs–Ringer bicarbonate buffer and ethanol were purchased by Sigma-Aldrich (St. Louis, MO, USA). Witepsol E85 was supplied by Cremer Oleo (Hamburg, Germany); Gelucire 44/14 was kindly provided by Gattefossé SAS (Saint-Priest, France). Acetonitrile was bought from Merck (Darmstadt, Germany). UDCA-AZT was synthesized as previously described [22]. Fetal bovine serum (FBS) was acquired from Life Technologies Italia (Monza, Italy). Fresh pig small intestines were obtained from the local slaughterhouse, from healthy animals slaughtered for the commercial meat production.

Preparation of polymeric nanoparticles

SS13 nanoparticles (SS13NP) were prepared using an o/w emulsification-solvent evaporation method [23]. Briefly, SS13 (6.4 mg) was dispersed in 4 mL DCM, and then PLGA (2.5% w/v) was added. The organic phase was dropped into 10 mL of MilliQ water containing 1% (w/v) of PVA with continuous stirring, and the obtained pre-emulsion was homogenized with a probe sonicator (Vibra Cell, VC 50, Sonics and Materials, Danbury, CT, USA) for 5 min at 60% amplitude. The resulting emulsion was placed under magnetic stirring at room temperature for 3 h to evaporate the DCM. Unloaded nanoparticles (NP) were prepared by employing the same procedure.

Analysis of particle size, polydispersity and zeta potential

The photon correlation spectroscopy (PCS), employing a Coulter Submicron Particle Sizer N5 (Beckman-Coulter Inc. Miami, FL, USA), was used to determine the particle size

and the polydispersity index (PDI) of SS13NP and NP. Three samples of nanodispersions were prepared, and each formulation was analyzed three times ($n = 9$). Zeta potential was measured with a Zetasizer Nano ZS (Malvern Instruments, Malvern, UK), on a 0.1 mg/mL suspension of SS13NP or NP in Milli-Q water at room temperature. The results were expressed as mean ± standard deviation (SD).

Physical stability studies

The influence of time and storing conditions on the physical stability of SS13NP and NP in dispersion was evaluated by determining the particle diameter and PDI of formulations stored at 25 °C or 4 °C, at 7, 15, 30, 60, and 90 days after preparation.

Morphological characterization by transmission electron microscope (TEM)

The morphology of SS13NP and NP was observed by a Tecnai G2 F20 Twin TMP (FEI Company, Dawson Creek, Hillsboro, OR, USA). For the sample preparation, 20 µL of SS13NP and NP dispersions was put on carbon film copper grids (ultra-thin (< 3 nm) Holey Carbon Film; 400 Mesh) and dried overnight at room temperature. TEM images were obtained by using a Digital Micrographfrom Gatan and TIA software.

Fourier transform infrared spectrometry analysis

To investigate the chemical structure of SS13NP, the Fourier transform infrared spectrometry (FTIR) (Avatar 320 FT-IT, Thermo Nicolet, Madison, WI, USA) was employed. For comparison, FTIR spectra of NP, SS13, SS13NP, and a physical mixture of NP with SS13 (prepared with the same drug amount of SS13NP) were recorded by EzOminic version 6.0 software. After preparation, the dispersions were dried at room temperature to have a powder material. The KBr pellet method was used to prepare samples.

Determination of the encapsulation efficiency

The encapsulation efficiency (EE) was determined by an indirect method evaluating the amount of unloaded SS13. For this purpose, 1 mL of SS13NP was centrifuged at 3000 rpm for 10 min, and the obtained precipitate was washed and centrifuged three times with MilliQ water. The final colored precipitate was then dissolved in acetonitrile (10 mL), and after centrifugation at 14,000 rpm for 10 min, the concentration of SS13 in the filtrate was detected by HPLC [12]. The encapsulation efficiency (EE) was calculated according to the following equation [24]:

$$EE\ (\%) = \frac{SS13\ in\ SS13NP - free\ SS13}{SS13\ in\ SS13NP} \times 100$$

where *SS13 in SS13NP* is the total amount of SS13 in the SS13NP dispersion, and *free SS13* is the amount of SS13 precipitate. The results are the average of three determinations.

The total amount of SS13 in the SS13NP dispersion was determined as follows: an exact amount of SS13NP (50 µL) was added to 950 µL of acetonitrile. The resulting suspension was vortexed for 1 min and centrifuged at 14,000 rpm for 10 min to extract SS13; the supernatant was analyzed using the HPLC method previously described [12]. Two extractions were sufficient.

In vitro drug release test

In vitro release studies were carried out as previously reported [12], due to the very poor solubility of SS13 in buffers simulated the intestinal pHs. An aliquot of SS13NP containing 0.12 mg of SS13 was placed in 15 mL of PBS containing 50% v/v FBS (FBS/PBS) stirred at 80 rpm in a shaker incubator (SKI 4 Shaker Incubator, Argo Lab, Carpi, Italy) at 37 ± 0.5 °C for 24 h. At predetermined time points, the medium (0.5 mL) was withdrawn by a syringe equipped with a filter (Corning syringe filters, regenerated cellulose membrane, diameter 4 mm, pore size 0.2 µm; Merck KGaA, Darmstadt, Germany) and replaced with the fresh FBS/PBS. The samples were diluted with acetonitrile before the HPLC analysis [12]. In vitro release studies were performed in triplicate ($n = 3$) and the results were expressed as a percentage.

Ex vivo permeation studies on pig intestinal mucosa

The ex vivo permeation test was carried out as previously described [12]. Briefly, the excised pig intestinal mucosa was fixed on a modified 12-well cell culture plates, appropriately made in our lab (project INCREASE SARDINIA 2016–17, protocol number 31351, University of Sassari), with the basolateral surface in contact with 5 mL of Krebs–Ringer bicarbonate buffer (pH 7.4). Then, an aliquot of SS13NP dispersion, raw SS13 mixed with NP dispersion (SS13 + NP), and raw SS13 dispersion in 2% w/v PVA solution, containing 0.06 mg of SS13, was applied to the apical surface of mucosa. The plates were shaken at 150 rpm and 25 °C for 180 min (SKI 4 Shaker Incubator, Argo Lab, Carpi, Italy); at different time points (30, 60, 120, and 180 min), the buffer was withdrawn and evaporated to dryness. SS13 permeated was extracted with acetonitrile and quantified by HPLC [12]. At the same time, the dispersion remained on mucosa was recovered, evaporated to dryness and treated with acetonitrile; then, the amount of SS13 unpermeated was measured by HPLC. The mucosa fragment was washed, dipped into

DCM and homogenized; after centrifugation, the supernatant was evaporated to dryness and mixed with acetonitrile. The acetonitrile solution was analyzed by HPLC for quantifying the SS13 remained inside the mucosa.

The experiment was performed in triplicate for each time point. The results were expressed as percentage with respect to the amount of SS13 in the dispersions.

In vivo studies

Preparation of lipid nanoparticles

SS13SLN were prepared and characterized as reported in a previous article [12]. Briefly, Witepsol E85 and Gelucire 44/14 (mass ratio 5:4; 200 mg) and SS13 (6.4 mg) were dissolved in 4 mL of DCM. Then, 10 mL of PVA aqueous solution (2% w/v) was poured into the organic phase under magnetic stirring; then the emulsion was sonicated for 90 s at 70% amplitude (Vibra Cell, VC 50, Sonics and Materials, Danbury, CT, USA) and stirred for 3 h at room temperature for removing the organic solvent. The SLN dispersion was centrifuged at 4000 rpm for 5 min to precipitate SS13, eventually free. Unloaded SLN (SLN) were similarly prepared. The SS13SLN had a size of 247.1 ± 19.8 μm and PDI of 0.772 ± 0.051 whereas SLN had 141.8 ± 12.0 μm diameter and 0.213 ± 0.020 PDI [12].

Pharmacokinetic studies

One mg/mL SS13 solution in DMSO was diluted in ethanol up to 0.333 mg/mL as SS13 final concentration. Male Sprague–Dawley rats (200–250 g; Charles River Laboratories, Italy) were randomly subdivided into nine groups (4 rats/group). One group received 0.2 mg (1 mg/kg) of SS13 as 0.6 mL of the drug formulation via a femoral intravenous infusion at a rate of 0.1 mL/min for 6 min. The second group received, in the same way, 0.6 mL of the vehicle (the mixture of DMSO and ethanol). The third group received 0.6 mg (3 mg/kg) of raw SS13 mixed with palatable food to induce the oral assumption by the rats fasted for 12 h. The fourth and fifth groups received orally by gavage 0.6 mg of SS13 (3 mg/kg), contained in 1 mL of SS13NP or SS13SLN, respectively. The sixth and seventh groups received by gavage 1 mL of unloaded NP or SLN samples, respectively. Finally, the eighth and ninth groups received orally by gavage 0.6 mg of raw SS13 mixed with unloaded NP and SLN (1 mL), respectively (Table 1).

The rats were anaesthetized during all the time required for experimental procedures. Blood samples (100 μL) were collected at fixed time points within 240 min after the end of infusions or oral administrations. As a control, a blood sample (100 μL) was collected by each rat before the drug or vehicle administration. The control and vehicle samples were immediately added to 300 μL of ice-cold CH_3CN, whereas the samples containing the drug were immediately added to 200 μL of ice-cold CH_3CN, and then 100 μL of internal standard (400 μM UDCA-AZT) was further inserted. The samples were centrifuged at 14,000 × g for 5 min, and then about 300 μL of supernatant was withdrawn and further centrifuged. Finally, 10 μL was analyzed via HPLC for SS13 quantification. The in vivo studies were carried out in accordance with current Italian legislation (D.L. 26/2014) that allows experimentation on laboratory animals only after the approval by Ministry of Health (Rome, Italy; protocol n: 793/2018-PR), and in strict accordance with the European Council Directives (n. 2010/63/EU) on animal use in research. The number of animals/group to reach significance has been calculated by G-power software (ANOVA, fixed effect, one-way). Any effort has been done to reduce the number of animals and their suffering.

The HPLC apparatus consisted of a modular system (model LC-10 AD VD pump and model SPD-10A VP variable wavelength UV – vis detector; Shimadzu, Kyoto, Japan)

Table 1 Summary of in vivo experimental groups

Group	Treatment	Administration route	Dose or amount
1	SS13	Femoral intravenous infusion	0.2 mg (1 mg/kg) dissolved in 0.6 mL of DMSO/ethanol mixture
2	DMSO/ethanol mixture (i.e. group 1 vehicle)	Femoral intravenous infusion	0.6 mL
3	SS13 (raw material)	Oral (added to palatable food)	0.6 mg (3 mg/kg SS13)
4	SS13NP	Oral (gavage)	0.6 mg SS13 (3 mg/kg SS13)
5	SS13SLN	Oral (gavage)	0.6 mg SS13 (3 mg/kg SS13)
6	NP	Oral (gavage)	1 mL unloaded NP
7	SLN	Oral (gavage)	1 mL unloaded SLN
8	SS13 + NP	Oral (gavage)	0.6 mg (3 mg/kg SS13); 1 mL unloaded NP
9	SS13 + SLN	Oral (gavage)	0.6 mg (3 mg/kg SS13); 1 mL unloaded SLN

and an injection valve with 20 µL sample loop (model 7725; Rheodyne, IDEX, Torrance, CA, USA). Separations were performed at room temperature on a reverse phase column Hypersil BDS C-18 (150 × 4.6 mm, 5 µm), equipped with a guard column packed with the same Hypersil material. The detector was set at 254 nm; the mobile phase was an isocratic mixture of water and acetonitrile at a ratio of 60:40 (v/v). Data acquisition and processing were performed on a personal computer using CLASS-VP Software, version 7.2.1 (Shimadzu Italia, Milan, Italy). The retention times of SS13 and UDCA-AZT were 3.8 min and 7.8 min, respectively. The chromatographic precision for SS13 dissolved in a water-acetonitrile mixture (25:75 v/v) was evaluated by repeated analysis ($n = 6$) of the same sample (25 µM or 15.8 µg/mL), and it is represented by the relative standard deviation (RSD) value of 0.88% referred to peak areas. The calibration curve of peak areas versus concentration was generated in the range 0.1 to 60 µM (0.06 to 37.9 µg/mL) for SS13 dissolved in the water-acetonitrile mixture (25:75 v/v) and appeared linear ($n = 10$, $r = 0.996$, $P < 0.0001$). About the blood samples, recovery experiments were performed comparing the peak areas extracted from a blood test sample of 25 µM (15.8 µg/mL) SS13 at 4 °C ($n = 4$) with those obtained by the injection of an equivalent concentration of the analyte dissolved in a water-acetonitrile mixture (25:75 v/v). The average recovery ± SD of SS313 from whole blood was 49.8 ± 1.6%. SS13 concentrations were therefore referred to peak area ratio with respect to the internal standard UDCA-AZT. The precision of the method based on the peak area ratio was represented by the RSD value of 1.28%. The calibration curve of SS13 extracted from whole blood at 4 °C was constructed by using nine different concentrations ranging from 0.3 to 60 µM (0.19 to 37.9 µg/mL) and appeared linear ($n = 9$, $r = 0.994$, $P < 0.0001$). The HPLC analysis of the control samples evidenced the absence of peaks interfering with those of the drug and the internal standard. Similarly, no peaks were evidenced at the retention time of the drug and internal standard by the HPLC analysis of the blood samples collected from the rats that received the vehicles (including the unloaded nanoparticles) related to intravenous and oral administrations.

The apparent first-order kinetic profile of SS13 concentration in the bloodstream during the time after the infusion was reported as exponential decay and confirmed by linear regression of the log concentration values versus time (semilogarithmic plot). The SS13 in vivo elimination constant (k_{el}) and half-life ($t_{1/2}$) were calculated from the slope of the semilogarithmic plot. The area under concentration curve (AUC, $\mu g \cdot mL^{-1} \cdot$ min) was calculated by the trapezoidal method within 240 min.

The clearance (CL) and distribution volume (V_d) values were calculated as the ratios "dose/AUC" and "CL/k_{el}," respectively.

The AUC values referred to each orally administered treatment were calculated by the trapezoidal method within 240 min. The absolute bioavailability values of SS13, referred to the oral administered free drug or samples NP SS13 and SLN SS13, were obtained as the ratio between their oral AUC values and AUC of the intravenous administration of the drug, normalized with respect to their doses, according to the following equation [25]:

$$F = \frac{AUC_{oral}}{AUC_{IV}} \cdot \frac{dose_{IV}}{dose_{oral}}$$

For NP SS13 and SLN SS13, the values of $dose_{oral}$ were referred to the encapsulated drug. All graphs and related calculations were obtained using Graph Pad Prism software, version 7 (GraphPad Software Incorporated, La Jolla, CA, USA).

Statistical analysis

The statistical analysis of data was performed using the GraphPad Prism 8.0 software (GraphPad Software, Inc., San Diego, CA, USA). Mann–Whitney or Kruskal–Wallis tests were used; the differences were considered statistically significant at $P < 0.05$.

Results and discussion

Analysis of particle size, polydispersity and zeta potential

NP and SS13NP showed size around 280 nm (Table 2): the drug loading did not lead to differences in particle size ($P > 0.05$), while it increased the PDI ($P < 0.05$), although still indicative of a monodisperse system with narrow distribution [26].

The size of SS13NP was not significantly different from SS13SLN (247.1 ± 19.8 µm), whereas the PDI was very low (SS13SLN PDI: 0.772 ± 0.051) [12].

Considering that size is one of the main factors affecting cellular uptake, a size < 300 nm allows nanoparticles to diffuse through the mucus and to take by enterocytes [6, 10]; it results that SS13NP has a suitable diameter for oral drug delivery because.

SS13NP and NP showed a slightly negative charge (Table 2), not affected by the loading of SS13, having a negative zeta potential (−9.24 ± 0.84 [12]) ($P > 0.05$). Furthermore, their zeta potential is not statistically different from that of SS13SLN (−13.82 ± 2.44 mV [12]) and SLN (−17.13 ± 2.51 mV [12]) ($P > 0.05$).

Table 2 Size, PDI, and zeta potential of nanoparticles prepared

Sample	Particle size (nm ± SD)	PDI ± SD	Zeta potential (mV)
NP	279.20 ± 5.80	0.062 ± 0.020*	−13.8 ± 0.7
SS13NP	283.40 ± 16.31	0.109 ± 0.038*	−15.1 ± 0.5

Results are expressed as mean ± SD

*$P < 0.05$

Physical stability studies

The mean diameter of both nanodispersions did not change significantly over time ($P > 0.05$) regardless of the storage temperature (Fig. 1), whereas the PDI of SS13NP alone increased from 0 to 7 days ($P < 0.05$) at 25 °C then remained stable under 0.4, characteristic of the moderate polydisperse distribution [26]. When stored at 4 °C, a statistical increase was observed after 90 days ($P < 0.05$), but the value reached 0.22. Therefore, SS13NP had high stability in dispersion and should be preferentially stored at 4 °C.

Morphological characterization by transmission electron microscope (TEM)

NP showed a spherical shape with a particle size ranging from 300 up to 50 nm for the smallest ones; SS13NP were almost identical in size to NP (Fig. 2). Moreover, it could be observed the presence, around but also inside even smaller particles (< 10 nm) and irregular shape, probably attributable to SS13.

The morphology of SS13NP was similar to SS13SLN, which appeared as single spherical particles with some larger in size [12].

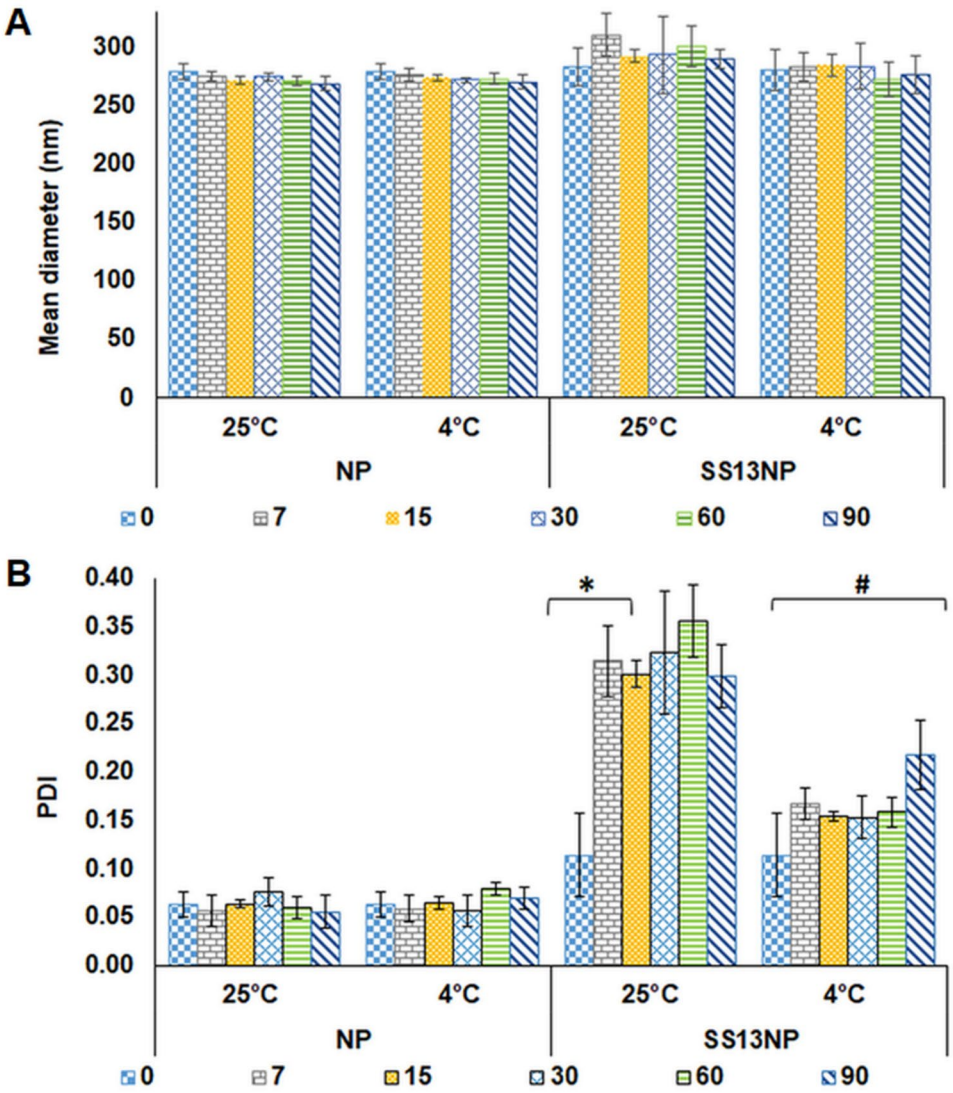

Fig. 1 Physical stability of NP and SS13NP dispersions. **A** Mean diameter (nm) and **B** PDI were measured for 90 days after preparation when stored at 4 and 25 °C. *$P < 0.05$ #0 vs 7 days; $P < 0.05$ 0 vs 90 days

Fourier transform infrared spectrometry analysis

Figure 3 shows the FTIR spectra of NP, SS13NP, SS13 alone, and in a physical mixture with NP. The spectrum of NP shows (*i*) the large band at 3200–3550 cm^{-1} due to the O–H stretching of PVA [27]; (*ii*) the peaks between 2840 and 3000 cm^{-1} linked to C–H stretching of both PVA and PLGA [16, 27]; (*iii*) and at 1700–1800 cm^{-1} due to the C=O stretching of both polymers [16, 27].

As reported in our previous work, the SS13 spectrum is characterized by peaks at 1647–1597 cm^{-1} and 1540–1487 cm^{-1} due to C–C stretching vibrations in the aromatic ring [12]. These peaks have very low intensity in the SS13NP spectrum that is almost superimposable to that of NP. On the contrary, the characteristic peaks of SS13 are intense in the physical mixture like SS13 alone. These results confirm the presence of a small amount of free SS13, as observed by TEM.

Determination of the encapsulation efficiency

The total amount of SS13 determined in SS13NP was 0.64 ± 0.03 mg/mL corresponding to $100 \pm 3.01\%$ of SS13 used for the preparation. This excludes the degradation or loss of the drug during the preparation process [24]. The EE was found to be $54.31 \pm 6.66\%$, different from the $100.00 \pm 3.11\%$ previously evidenced for SS13SLN [12]; this means that about half of SS13 was loaded into the polymeric nanoparticles and the remaining was free in the dispersion, probably stabilized by PVA [28]. This result matches with previous evidence indicating that PVA-PLGA nanoparticles have a limited ability to load drugs with low solubility and log *P* value [14].

In vitro drug release test

Figure 4 reports the release kinetics of SS13 from SS13NP: $11.05 \pm 6.69\%$ of the SS13 content was found in the dissolution medium after 2 h and 14.92 1.76% after 24 h. Therefore, SS13NP showed slower release than SS13 and SS13SLN ($P < 0.05$). As previously reported, 35% and 24% of SS13 dissolved in the medium within 2 h when SS13 alone and SS13SLN were tested, respectively; then, all profiles have reached the plateau [12].

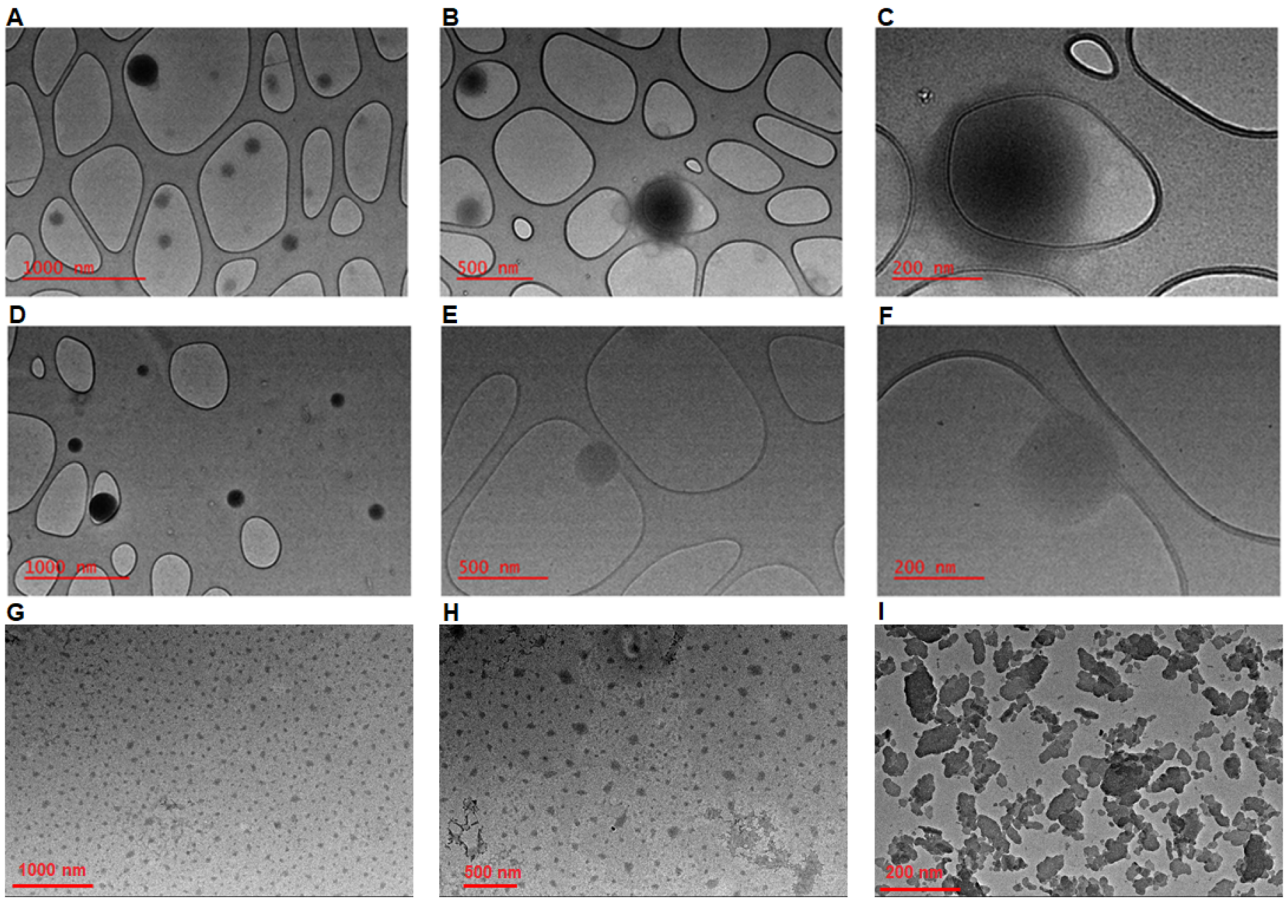

Fig. 2 TEM pictures of **A–C** NP, **D–F** SS13NP and, as comparison, **G–H** SS13SLN, and **I** SLN [12]

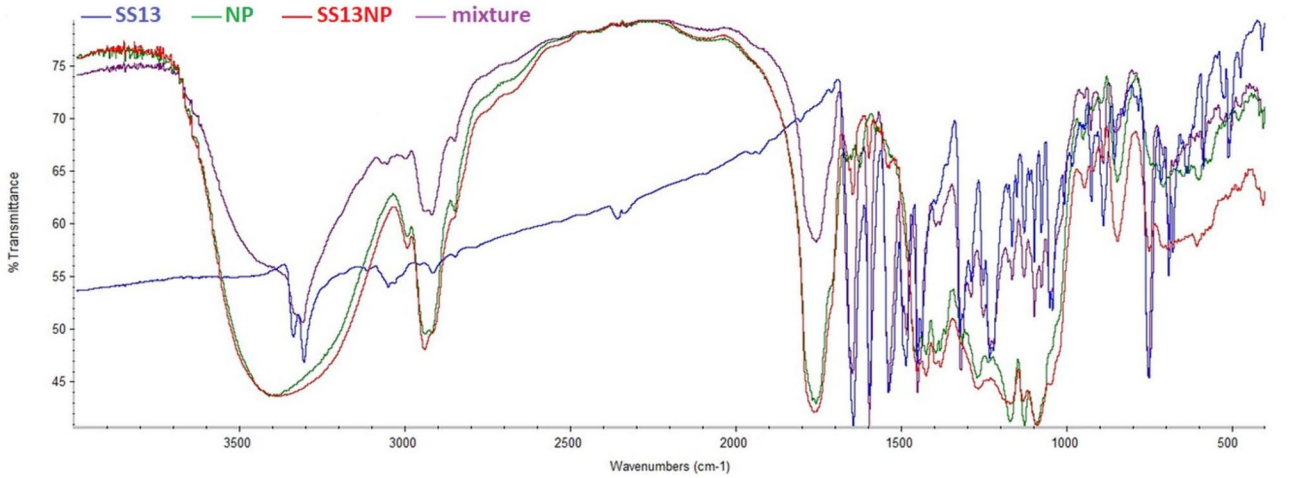

Fig. 3 FT-IR spectra of SS13, NP, SS13NP, and a physical mixture of NP with SS13

This different behavior may be attributed to the solubilizing effect of both serum proteins and Gelucire 44/14.

Ex vivo permeation studies on intestinal mucosa

During the ex vivo permeation test, the SS13 amount that remained on the intestinal mucosa, penetrated inside the mucosa, and permeated was quantified; the results are reported in Fig. 5. It can be observed that, when SS13NP was tested, the amount of SS13 remained on the intestinal mucosa decreased during the time due to the slow, but progressive penetration of the drug into the excised tissue. SS13NP increased the permeation of SS13 loaded after 120 min compared to SS13 alone ($P < 0.05$). On the contrary, SS13 when mixed with NP was not able to permeate after 120 min. Nevertheless, SS13NP showed a lower capability to increase the permeation of SS13 than SS13SLN ($P < 0.05$). This could be due to the Gelucire 44/14 that, as a nonionic water-dispersible surfactant, may improve the intestinal absorption [12].

Pharmacokinetic studies

SS13 was previously evidenced as a compound characterized by both poor aqueous media solubility and low lipophilicity [12]. Due to these specific chemical-physical properties, a DMSO and ethanol mixture (33.3:66.7 v/v, respectively) was required for the intravenous administration of SS13.

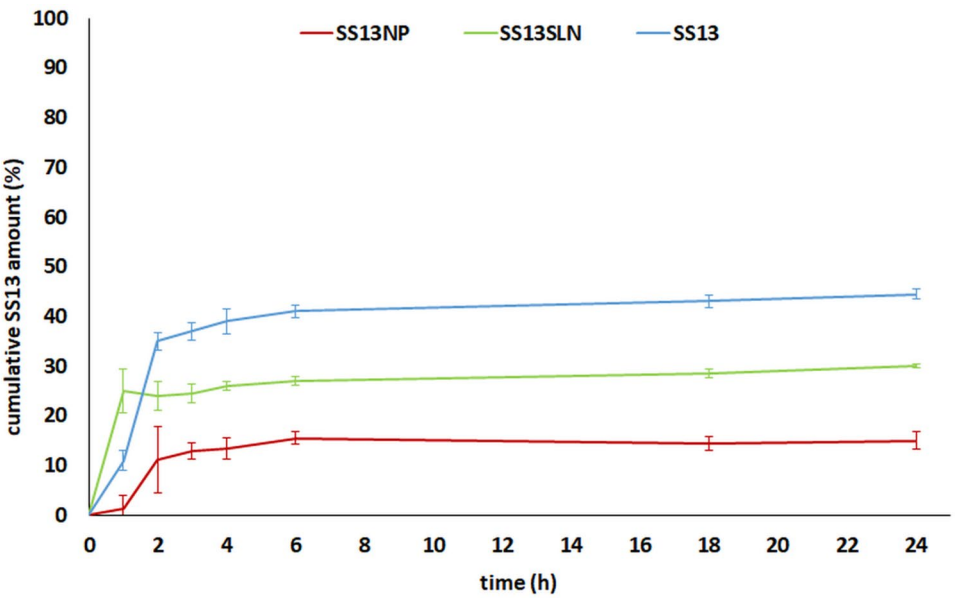

Fig. 4 In vitro release profile of SS13 from SS13NP. For comparison, data from SS13 and SS13SLN, previously published, have been reported [12]. $P < 0.05$ SS13NP vs SS13 and SS13NP vs SS13SLN

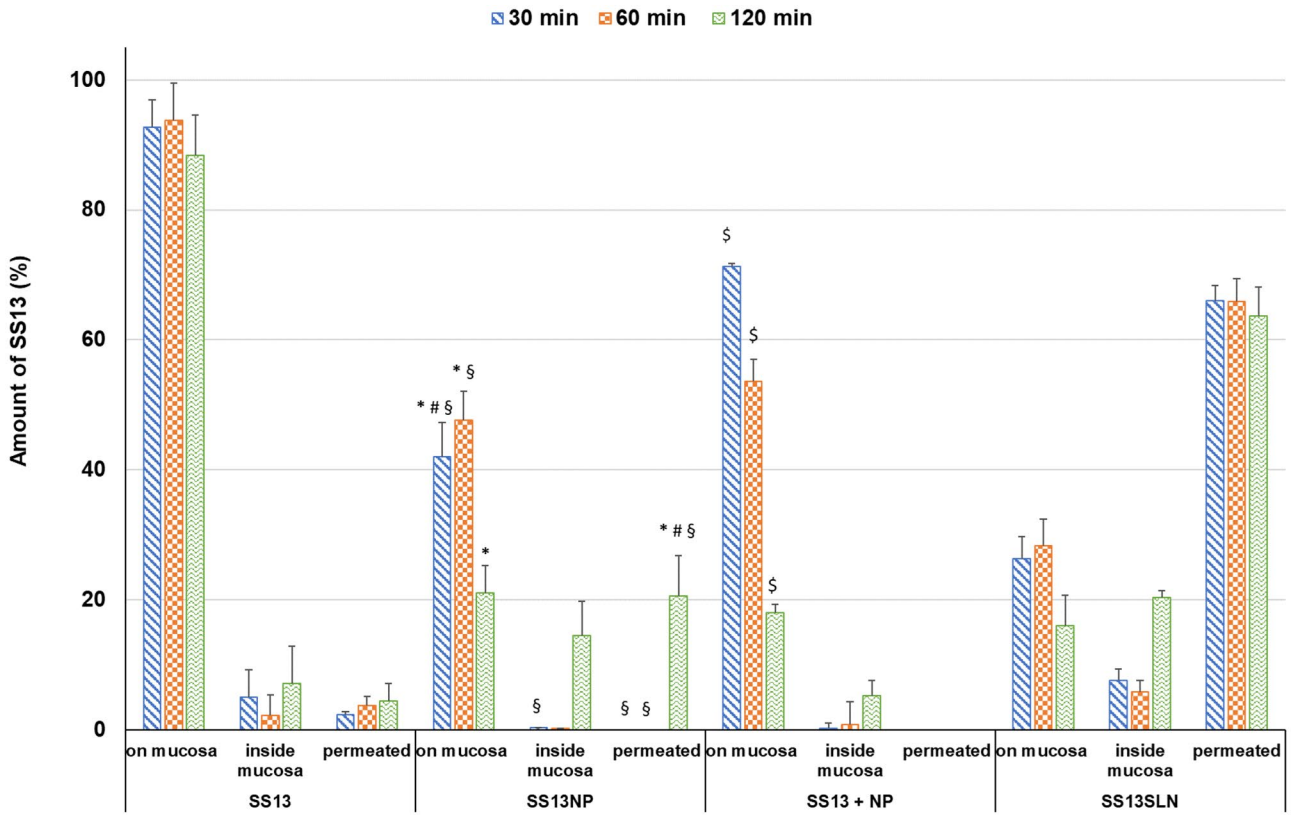

Fig. 5 Ex vivo distribution of SS13 at different time points (30, 60, and 120 min) during the permeation test of SS13NP and SS13 + NP through the intestinal mucosa ($n = 3$). For comparison, data from SS13 and SS13SLN, previously published, have been reported [12]. *$P < 0.05$ SS13NP vs SS13; #$P < 0.05$ SS13NP vs SS13 + NP; §$P < 0.05$ SS13NP vs SS13SLN; $$P < 0.05$ SS13 + NP vs SS13

This solvent mixture allowed to perform the femoral intravenous infusion to rats of 0.2 mg of SS13 (1 mg/kg) at a rate of 0.1 mL/min for 6 min and did not interfere with the HPLC analysis of the drug and its internal standard from the blood samples. The dose of 1 mg/kg was chosen taking into account that it appeared suitable to define the pharmacokinetic profile, by HPLC–UV analysis, of previously studied drugs [29–32]. In this case, the highest SS13 concentration detected in whole blood at the end of infusion was 30.9 ± 4.5 µg/mL, and it decreased during the time (Fig. 6), with an apparent first-order kinetic confirmed by the linearity of the semilogarithmic plot reported in the inset of Fig. 6 ($n = 7$, $r = 0.973$, $p < 0.001$), and a half-life ($t_{1/2}$) of 28.7 ± 2.9 min. The pharmacokinetic data (Table 3) indicate a clearance (CL) value of 0.71 ± 0.04 mL·min^{-1}·kg^{-1} and a volume of distribution (V_d) value of 29.8 ± 4.7 mL·kg^{-1}.

The data reported in Table 3 indicate that a 0.2 mg (1 mg/kg) dose of SS13 allowed to obtain a C_0 value of about 30 µg/mL (i.e., 50 µM) in the rat bloodstream. This value is about five times higher than the C_0 values we previously measured following the intravenous administration of the same dose of anti-ischemic agents [29, 30], an antibiotic [31], or an antiviral agent [32]. Accordingly, the intravenous administration of 2.5 mg of a geraniol prodrug allowed to obtain a C_0 value of about 70 µg/mL [33]. The relatively

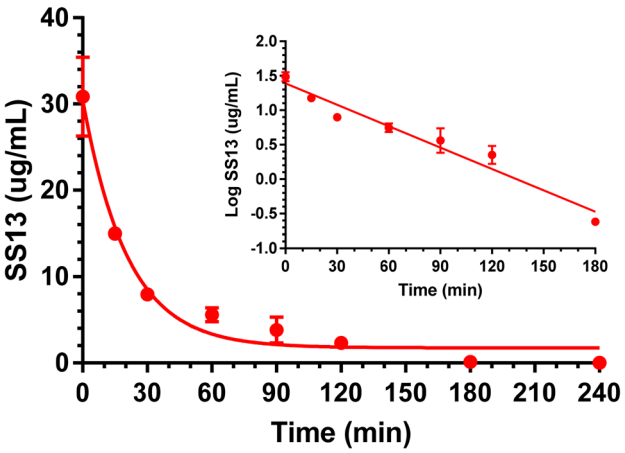

Fig. 6 Plasma elimination profile of SS13 intravenously infused to rats at 0.2 mg (1 mg/kg) dose. The elimination followed an apparent first-order kinetic, confirmed by the semilogarithmic plot reported in the inset ($n = 7$, $r = 0.973$, $P < 0.001$). The calculated half-life of SS13 was 28.9 ± 2.1 min. All data are expressed as the mean ± SD of four independent experiments

Table 3 Pharmacokinetic parameters of SS13 after intravenous administration of a 0.2 mg (1 mg/kg) dose to rats

C_0 (μg/mL)	AUC (μg·mL^{-1}·min)	k_{el} (1/min)	$t_{1/2}$ (min)	CL (mL·min^{-1}· kg^{-1})	Vd (mL/kg)
30.9 ± 4.5	1120 ± 58	0.024 ± 0.002	28.7 ± 0.9	0.71 ± 0.04	29.8 ± 4.7

Data are reported as mean ± SD ($n = 4$)

C_0 concentration at the end of infusion, *AUC* area under concentration, k_{el} elimination rate constant, $t_{1/2}$ half-life, *CL* clearance, *Vd* volume of distribution

high C_0 value obtained by SS13 intravenous administration suggests the poor aptitude of this compound to migrate from the bloodstream to peripheral tissues, also evidenced by its relatively low distribution volume (V_d about 30 mg/kg), which appears as one of the lowest V_d values reported in the literature for rats [34, 35]. These data allow hypothesizing that SS13 can have great difficulties to permeate across physiologic barriers, as confirmed by the demonstration that any amount of SS13 was detected by HPLC analysis in the blood of rats following the oral administration of 0.6 mg (3 mg/kg) of the raw compound (Table 4). This finding is in line with the demonstration that SS13 is insoluble in simulated gastrointestinal media [12].

Appropriate formulations appear therefore required to potentiate the ability of SS13 to permeate across physiologic barriers. We have previously demonstrated that the SS13SLN were able to increase by three orders of magnitude (from about $4.5 \cdot 10^{-8}$ cm/s to about $8.5 \cdot 10^{-5}$ cm/s) the permeability coefficient across pig intestinal mucosa of this drug, in comparison with its raw form [12]. Moreover, SS13NP appears capable of increasing the ability of SS13 to permeate across the same mucosa although to a lesser extent.

Accordingly, detectable amounts of SS13 were found in the bloodstream of rats following the oral administration of SS13NP or SS13SLN containing 0.6 mg (3 mg/kg) of the loaded drug, as reported in Fig. 7. The dose of 3 mg/kg was chosen taking into account that the maximum volume accepted for oral administration to rats of liquid formulations is 1 mL. The SS13 amount contained in SS13NP and SS13SLN formulations was 0.6 mg/mL. Following their oral administration, the SS13 concentrations showed C_{max} values of 2.47 ± 0.14 μg/mL at 20 min for SS13NP and 1.30 ± 0.15 μg/mL at 60 min for SS13SLN (Table 4). The absolute bioavailability values of SS13 were 12.67 ± 1.43% and 4.38 ± 0.39% after the oral administration of SS13NP and SS13SLN, respectively (Table 4), as calculated by the AUC values reported in Tables 1 and 2 and taking into account the amounts of the encapsulated drug (54.3% for SS13SLN and 100.0% for SS13NP [12]). On the other hand, the oral administration of raw SS13 (3 mg/kg) mixed with unloaded NP or SLN samples did not allow to detect any amount of the drug in the bloodstream of the rats (Table 4).

The in vivo results indicate SS13NP as the nanoparticulate system characterized by the higher ability to improve the oral bioavailability of SS13 (showing also higher C_{max} value in a shorter time) compared with SS13SLN. This different in vivo behavior does not seem related to the size, zeta potential, and morphology of the samples, and instead, it could be mainly related to their different composition: in fact, both polymeric and lipid nanoparticles had the same size (283.40 ± 16.31 nm and 247.1 ± 19.8 nm of SS13NP and SS13SLN, respectively) and shape (spherical) that are currently known as the main nanoparticle properties affecting the oral drug bioavailability [6, 9]. The influence of the zeta potential on barrier permeation can be also excluded (−15.1 ± 0.5 mV and −13.82 ± 2.44 mV of SS13NP and SS13SLN, respectively). SLN are known as carriers useful for oral delivery of BCS IV drugs because they are effective in overcoming the scarce solubility and permeability of the drug that affects the oral bioavailability, mainly promoting cell uptake and lymphatic transport [18]. As previously demonstrated, after internalization in the intestinal cells, SLN

Table 4 Pharmacokinetic parameters of SS13 after oral administration of a 0.6 mg (3 mg/kg) dose to rats as raw drug and mixed or encapsulated in the nanoparticles

Formulation	C_{max} (μg/mL)	T_{max} (min)	AUC (μg·mL^{-1}·min)	F (%)
SS13	0	0	0	0
SS13 + NP	0	0	0	0
SS13 + SLN	0	0	0	0
SS13NP	2.47 ± 0.14	20	227 ± 14	12.67 ± 1.43
SS13SLN	1.30 ± 0.15	60	147 ± 8	4.38 ± 0.39

Data are reported as mean ± SD ($n = 4$)

C_{max} highest concentration following the administration, T_{max} time corresponding to C_{max}, AUC area under concentration, *F* absolute bioavailability (for SS13NP and SS13SLN, the value of F was calculated considering the amount of encapsulated SS13 that was 54.3% for SS13NP and 100% for SS13SLN)

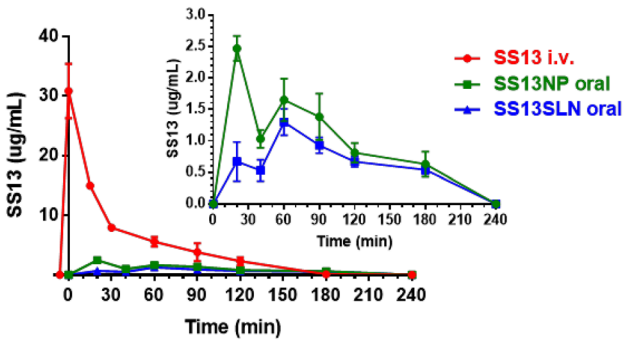

Fig. 7 SS13 profile in the bloodstream of rats related to the intravenous infusion of free drug (1 mg/kg) and oral administration loaded drug (3 mg/kg) in SS13NP and SS13SLN samples. All data are expressed as the mean ± SD of four independent experiments

could form chylomicrons and reach the intestinal lymphatic vessels and, then, the systemic circulation [13]. On the other hand, in common with all PLGA nanoparticles, SS13NP could improve drug absorption and transport through the intestinal epithelium after oral administration due to the high passive and active uptake by the enterocytes and/or M-cells in Peyer's patches and by the follicles of the gut-associated lymphoid tissue (GALT) [14, 15]. Finally, it is worth noting that the present results provide the first in vivo evidence of the possible effectiveness of SS13NP to improve drug oral bioavailability. In view of the encouraging results, further studies will be conducted to evaluate whether this formulation can allow to reach in vivo effective concentrations of SS13N, also considering metabolic aspects.

Conclusion

SS13NP based on PLGA had a suitable size for oral administration (less than 300 nm), a spherical shape and a slightly negative charge similar to SS13SLN. On the contrary, they showed higher physical stability in dispersion, but lower encapsulation efficiency (54.31 ± 6.66%) than SS13SLN (100.00 ± 3.11%). Contrary to the ex vivo results, SS13NP showed a greater ability (about three times) to increase the oral bioavailability of SS13 concerning SS13SLN. These in vivo results confirm that the chemical composition of nanoparticles significantly affects the in vivo fate of a BCS IV drug unable to cross the intestinal barriers alone. Moreover, it could be assumed that the transport mechanism of PLGA nanoparticles are more efficient and rapid in allowing drug absorption and achieving systemic circulation than SLN.

Acknowledgements The authors acknowledge the GAUSS (Grandi Attrezzature Università di Sassari) core facility of the University of Sassari and Marzia Mureddu for TEM analysis.

Author contribution Elisabetta Gavini, Giovanna Rassu, and Paolo Giunchedi contributed to the study's conception and design. Material preparation, data collection, and analysis were performed by Antonella Obinu, Alessandro Dalpiaz, Luca Ferraro, and Carla Serri. Sandra Piras and Antonio Carta designed and synthesized the drug. Antonio Carta and Paolo Giunchedi acquired the funding. The first draft of the manuscript was written by Giovanna Rassu, and all authors commented on previous versions of the manuscript. All authors read and approved the final manuscript.

Funding This work was supported by the Sardinia Regional Government (FSC 2014–2020 programmes of Regione Autonoma della Sardegna; Grant numbers RASSR01499) and by the Foundation of Sardinia (Bando Fondazione di Sardegna – 2018–2020 e 2021 – Progetti di ricerca di base dipartimentali"; grant numbers J89J21015120005).

Data availability The datasets generated during and/or analyzed during the current study are available from the corresponding author upon reasonable request.

Declarations

Ethics approval All institutional and national guidelines for the care and use of laboratory animals were followed. This study was performed in accordance with the European Communities Council Directive of September 2010 (2010/ 63/EU). Approval was granted by the Ethics Committee of the University of Ferrara and by the Italian Ministry of Health (No 793/2018-PR).

Consent for publication All authors have read and agreed to the published version of the manuscript.

Competing interests The authors declare no competing interests.

References

1. Benet LZ, Broccatelli F, Oprea TI. BDDCS applied to over 900 drugs. AAPS J. 2011;13:519–47.
2. Kalepu S, Nekkanti V. Improved delivery of poorly soluble compounds using nanoparticle technology: a review. Drug Deliv Transl Res. 2016;6:319–32.
3. Committee for Medicinal Products for Human Use, EMA. ICH M9 guideline on biopharmaceutics classification system-based biowaivers. 2020. Available from: https://www.ema.europa.eu/en/documents/scientific-guideline/ich-m9-biopharmaceutics-classification-system-based-biowaivers-step-5_en.pdf. Accessed 3 Oct 2022.
4. Ghadi R, Dand N. BCS class IV drugs: highly notorious candidates for formulation development. J Controlled Release. 2017;248:71–95.
5. Ghosh S, Ghosh S, Sil PC. Role of nanostructures in improvising oral medicine. Toxicol Rep. 2019;6:358–68.
6. Wang Y, Pi C, Feng X, Hou Y, Zhao L, Wei Y. The influence of nanoparticle properties on oral bioavailability of drugs. Int J Nanomedicine. 2020;15:6295–310.
7. Nieto González N, Obinu A, Rassu G, Giunchedi P, Gavini E. Polymeric and lipid nanoparticles: which applications in Pediatrics? Pharmaceutics. 2021;13:670.
8. Plaza-Oliver M, Santander-Ortega MJ, Lozano MV. Current approaches in lipid-based nanocarriers for oral drug delivery. Drug Deliv Transl Res. 2021;11:471–97.
9. Åslund AKO, Vandebriel RJ, Caputo F, de Jong WH, Delmaar C, Hyldbakk A, Rustique E, Schmid R, Snipstad S, Texier I,

Vernstad K, Borgos SEF. A comparative biodistribution study of polymeric and lipid-based nanoparticles. Drug Deliv Transl Res. 2022;12:2114–31.
10. Guo S, Liang Y, Liu L, Yin M, Wang A, Sun K, Li Y, Shi Y. Research on the fate of polymeric nanoparticles in the process of the intestinal absorption based on model nanoparticles with various characteristics: size, surface charge and pro-hydrophobics. J Nanobiotechnology. 2021;19:32.
11. Banerjee A, Qi J, Gogoi R, Wong J, Mitragotri S. Role of nanoparticle size, shape and surface chemistry in oral drug delivery. J Control Release. 2016;238:176–85.
12. Obinu A, Porcu EP, Piras S, Ibba R, Carta A, Molicotti P, Migheli R, Dalpiaz A, Ferraro L, Rassu G, Gavini E, Giunchedi P. Solid Lipid Nanoparticles as formulative strategy to increase oral permeation of a molecule active in multidrug-resistant tuberculosis management. Pharmaceutics. 2020;12:1132.
13. Obinu A, Burrai GP, Cavalli R, Galleri G, Migheli R, Antuofermo E, Rassu G, Gavini E, Giunchedi P. Transmucosal solid lipid nanoparticles to improve genistein absorption via intestinal lymphatic transport. Pharmaceutics. 2021;13:267.
14. Shailender J, Ravi PR, Saha P, Dalvi A, Myneni S. Tenofovir disoproxil fumarate loaded PLGA nanoparticles for enhanced oral absorption: effect of experimental variables and in vitro, ex vivo and in vivo evaluation. Colloids Surf B Biointerfaces. 2017;158:610–9.
15. Sharma S, Parmar A, Kori S, Sandhir R. PLGA-based nanoparticles: a new paradigm in biomedical applications. TrAC Trends Anal Chem. 2016;80:30–40.
16. Nallamuthu I, Parthasarathi A, Khanum F. Thymoquinone-loaded PLGA nanoparticles: antioxidant and anti-microbial properties. Int Curr Pharm J. 2013;2:202–7.
17. Xie X, Tao Q, Zou Y, Zhang F, Guo M, Wang Y, et al. PLGA nanoparticles improve the oral bioavailability of curcumin in rats: characterizations and mechanisms. J Agric Food Chem. 2011;59:9280–9.
18. Talegaonkar S, Bhattacharyya A. Potential of Lipid Nanoparticles (SLNs and NLCs) in enhancing oral bioavailability of drugs with poor intestinal permeability. AAPS PharmSciTech. 2019;20:121.
19. Ji H, Tang J, Li M, Ren J, Zheng N, Wu L. Curcumin-loaded solid lipid nanoparticles with Brij78 and TPGS improved in vivo oral bioavailability and in situ intestinal absorption of curcumin. Drug Deliv. 2016;23:459–70.
20. Araújo F, Shrestha N, Shahbazi M-A, Fonte P, Mäkilä EM, Salonen JJ, et al. The impact of nanoparticles on the mucosal translocation and transport of GLP-1 across the intestinal epithelium. Biomaterials. 2014;35:9199–207.
21. Panigrahi KC, Patra ChN, Jena GK, Ghose D, Jena J, Panda SK, et al. Gelucire: a versatile polymer for modified release drug delivery system. Future J Pharm Sci. 2018;4:102–8.
22. Dalpiaz A, Paganetto G, Pavan B, Fogagnolo M, Medici A, Beggiato S, Perrone D. Zidovudine and ursodeoxycholic acid conjugation: design of a new prodrug potentially able to bypass the active efflux transport systems of the central nervous system. Mol Pharm. 2012;9:957–68.
23. Jin C, Bai L, Wu H, Song W, Guo G, Dou K. Cytotoxicity of paclitaxel incorporated in PLGA nanoparticles on hypoxic human tumor cells. Pharm Res. 2009;26:1776–84.
24. Nieto González N, Cerri G, Molpeceres J, Cossu M, Rassu G, Giunchedi P, Gavini E. Surfactant-free chitosan/cellulose acetate phthalate nanoparticles: an attempt to solve the needs of captopril administration in Paediatrics. Pharmaceuticals. 2022;15:662.
25. Simovic S, Heard P, Hui H, Song Y, Peddie F, Davey AK, Lewis A, Rades T, Prestidge CA. Dry hybrid lipid-silica microcapsules engineered from submicron lipid droplets and nanoparticles as a novel delivery system for poorly soluble drugs. Mol Pharm. 2009;6:861–72.
26. Estrada-Fernández AG, Román-Guerrero A, Jiménez-Alvarado R, Lobato-Calleros C, Alvarez-Ramirez J, Vernon-Carter EJ. Stabilization of oil-in-water-in-oil (O1/W/O2) Pickering double emulsions by soluble and insoluble whey protein concentrate-gum Arabic complexes used as inner and outer interfaces. J Food Eng. 2018;221:35–44.
27. Mansur HS, Sadahira CM, Souza AN, Mansur AAP. FTIR spectroscopy characterization of poly (vinyl alcohol) hydrogel with different hydrolysis degree and chemically crosslinked with glutaraldehyde. Mater Sci Eng C. 2008;28:539–48.
28. Xia D, Quan P, Piao H, Piao H, Sun S, Yin Y, Cui F. Preparation of stable nitrendipine nanosuspensions using the precipitation–ultrasonication method for enhancement of dissolution and oral bioavailability. Eur J Pharm Sci. 2010;40:325–34.
29. Dalpiaz A, Gavini E, Colombo G, Russo P, Bortolotti F, Ferraro L, Tanganelli S, Scatturin A, Menegatti E, Giunchedi P. Brain uptake of an anti-ischemic agent by nasal administration of microparticles. J Pharm Sci. 2008;97:4889–903.
30. Rassu G, Soddu E, Cossu M, Brundu A, Cerri G, Marchetti N, Ferraro L, Regan RF, Giunchedi P, Gavini E, Dalpiaz A. Solid microparticles based on chitosan or methyl-β-cyclodextrin: a first formulative approach to increase the nose-to-brain transport of deferoxamine mesylate. J Control Release. 2015;201:68–77.
31. Gavini E, Rassu G, Ferraro L, Generosi A, Rau JV, Brunetti A, Giunchedi P, Dalpiaz A. Influence of chitosan glutamate on the in vivo intranasal absorption of rokitamycin from microspheres. J Pharm Sci. 2011;100:1488–502.
32. Dalpiaz A, Fogagnolo M, Ferraro L, Capuzzo A, Pavan B, Rassu G, Salis A, Giunchedi P, Gavini E. Nasal chitosan microparticles target a zidovudine prodrug to brain HIV sanctuaries. Antiviral Res. 2015;123:146–57.
33. de Oliveira Junior ER, Truzzi E, Ferraro L, Fogagnolo M, Pavan B, Beggiato S, Rustichelli C, Maretti E, Lima EM, Leo E, Dalpiaz A. Nasal administration of nanoencapsulated geraniol/ursodeoxycholic acid conjugate: towards a new approach for the management of Parkinson's disease. J Control Release. 2020;321:540–52.
34. Djekic L, Janković J, Rašković A, Primorac M. Semisolid self-microemulsifying drug delivery systems (SMEDDSs): Effects on pharmacokinetics of acyclovir in rats. Eur J Pharm Sci. 2018;121:287–92.
35. Jin Y, Yu L, Xu F, Zhou J, Xiong B, Tang Y, Li X, Liu L, Jin W. Pharmacokinetics of active ingredients of salvia miltiorrhiza and carthamus tinctorius in compatibility in normal and cerebral ischemia rats: a comparative study. Eur J Drug Metab Pharmacokinet. 2020;45:273–84.